PHYSICAL REVIEW B VOLUME 56, NUMBER 12 15 SEPTEMBER 1997-II

Perpendicular magnetization in ultrathin electrodeposited cobalt films

J. L. Bubendorff, E. Beaurepaire, C. Mény, P. Panissod, and J. P. Bucher*
Institut de Physique et de Chimie des Matériaux de Strasbourg (IPCMS), Université Louis Pasteur, 23 rue du Loess, F-67037 Strasbourg Cedex, France

(Received 5 May 1997)

Electrodeposited ultrathin cobalt films on Au(111) covered with a protective copper film can show perpendicular magnetization exactly like their ultrahigh-vacuum-grown counterparts. At high deposition rates of cobalt, out-of-plane magnetization is stabilized in the thickness range from 2 to 8 atomic layers while low deposition rates favor in-plane magnetization at any thickness. The cobalt films possess hcp structure with the *c* axis perpendicular to the Au(111) plane. The technique is versatile and leads to quality standards comparable to those obtained by molecular-beam epitaxy, but at a much lower cost. [S0163-1829(97)51236-7]

Up to now, most of the knowledge on ultrathin magnetic films referred to molecular-beam epitaxy (MBE) techniques.[1] Although MBE techniques have reached a high degree of perfection, they rely on state of the art and costly equipment operating under an ultrahigh vacuum (UHV) and are sometimes not compatible with large scale productions of nanostructured materials. On the other hand, electrochemical deposition techniques are cheap, versatile, and allow a wide range of parameters to be adjusted. They are ideally adapted to the engineering of nanostructured advanced materials, such as superlattices, for superconducting and giant magnetoresistance applications.[2–4] In addition, innovative techniques can be developed[5,6] in which magnetic needles and multilayers are grown electrochemically in pores of membranes leading to structures with high aspect ratios impossible to realize by MBE and conventional lithography. The technique allows extensive control. For example, it has been shown recently that magneto-optic Kerr measurements can be used to monitor, *in situ*, the magnetization of electrodeposited cobalt films on copper during their growth.[7]

In this paper, we present a successful electrodeposition of a film [in this case Co/Au(111)] with a magnetization perpendicular to the film plane. This configuration is of considerable interest for technological applications (in particular magneto-optic data storage) and has been stabilized previously only on ultrathin epitaxial films grown in UHV.[8–13] We show how the magnetic anisotropy (the tendency of the magnetization to align along a given direction) of ultrathin, electrodeposited, cobalt films on Au(111) can be tuned continuously from in-plane to out-of-plane by carefully controlling the overpotential η during deposition ($\eta = U_{\text{applied}} - U_{\text{equilibrium}}$) in a beaker.

Gold substrates were prepared by vacuum evaporation of 100-nm-thick gold films onto freshly cleaved mica substrate. Each sample was then flame annealed for a few seconds and quenched in ultrapure water in order to remove any organic contaminants. This leads to (111) textured gold films with terraces 100 to 200 nm wide as verified by scanning tunnel microscopy (STM).[14] Electrochemical measurements were conducted in a 3 electrode cell under a potentiostatic mode, with a mercury sulfate electrode (MSE) as a reference and a Pt counter electrode. Solutions of 4×10^{-2} *M* $CoSO_4$ and 9×10^{-3} *M* Co were prepared with reagent grade Cl_2 chemicals in bidistilled water. No additives have been used and pH=4 is achieved by adding H_3BO_4 to the solution. Bulk deposition of cobalt is performed only after a high-quality gold Au(111) electrode has been identified by its characteristic $\sqrt{3}\times22$ reconstruction and dereconstruction peaks in the cyclic voltammograms (cyclic current-voltage curves).[15] In order to avoid possible perturbation by hydrogen release (the efficiency of Co electrodeposition is 96%), the quantity of deposited cobalt is measured during desorption only. Therefore, several adsorption-desorption cycles were performed before final deposition. The amount of deposited Co is obtained by integrating the Co dissolution peak over time while sweeping the electrode potential. As verified independently by Rutherford back-scattering (RBS) analysis, this technique allows control of the amount of deposited cobalt to within 0.1 AL (AL≡atomic layer). In order to induce widely different growth modes, a set of samples of thicknesses between 1 and 100 AL have been grown at overpotentials between η=0.18 and 0.68 V (Ref. 16) corresponding to deposition rates between 0.15 and 10 AL/s.

Although considerable progress has been made in understanding nucleation and growth at the solid-liquid interface, mainly on the basis of *in situ* STM experiments,[17,18] very little is known about how growth and structural parameters influence the magnetic properties of electrodeposited films. In an effort to understand growth and nucleation related magnetic properties, we analyzed the current transient immediately after the potential step [Fig. 1(a)]. The shapes of the curves in Fig. 1(a) are characteristic for diffusion limited three-dimensional growth in which the current raises to a maximum and decays to a final value defined by the diffusion limitation through the solution. Figure 1(b) shows the same data points in a reduced variable plot. By comparing with calculated data (continuous and dotted lines) by means of Ref. 17, we find that the first part of the curves, up to the maximum value of the current, are relevant for instantaneous nucleation (in which deposition is dominated by growth with no further nucleation) while at later times progressive nucleation sets in (in which new nuclei are continuously produced during the deposition process). As an example, a film grown within 10 s at η=0.18 V (corresponding to $t_{\text{Co}}\approx3$ AL) will be dominated by instantaneous nucleation, most probably occurring at atomic steps or defects of the Au(111) surface[19] and the first few AL's will be quite uniform. On the other

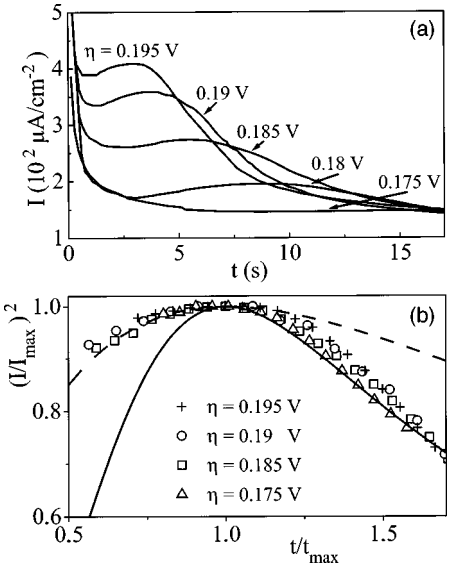

FIG. 1. (a) Current transient immediately after the potential step for various overpotentials η. The rapid increase of current at short time ($t<0.5$ s) is only due to capacitance charging of the double layer. (b) Normalized experimental data points compared to calculated curves for instantaneous (----) and progressive (—) nucleation. I_{max} corresponds to the maximum current reached at t_{max} on the current transient.

hand, the films obtained at $\eta=0.68$ V (high supersaturation) grow by continuously forming nuclei at any t_{Co}, leading first to a high density of disconnected islands with high crystallographic quality as seen by NMR (see below), and then to films with a fine granulation. Cobalt films have been covered *in situ* by an additional 30-AL-thick Cu film after addition of a 10^{-2} M $CuSO_4$ solution to the base solution. The Cu/Co/Au films have finally been removed from the solution and tested (*ex situ*) for their magnetic and structural properties. The Cu films provide a very efficient, pinhole-free protection of the Co films.

The local crystallographic structure of the buried Co films has been studied by zero-field nuclear magnetic resonance (NMR) at 1.5 K with a broadband automated spectrometer.[20] The NMR spectrum obtained for the Cu/Co(11 AL)/Au sample deposited at high overpotential and pH=4 is displayed in Fig. 2. Several characteristic features can be observed. At first the main line resonance frequency lies at about 226 MHz, corresponding to the resonance frequency of bulk hcp Co with a local magnetization direction perpendicular to the crystal c axes (the resonance frequency becomes 222 MHz when the magnetization is parallel to the c axes). This, together with the fact that this sample exhibits an in-plane magnetization, confirms the good quality of its crystallographic structure and the (0001) texture. The second feature is the shoulder at 217 MHz corresponding to fcc Co. Since for fcc Co the resonance frequency does not depend on the magnetization direction, using NMR will not tell us the texture of the fcc contribution. Both fcc and hcp frequencies are exactly like those observed for bulk Co, meaning that the strain in the Co film is nearly relaxed. For both high and low overpotentials, the content of fcc cobalt is the same and involves about 20% of the bulk Co atoms. The last feature is the lack of an NMR signal below 165 MHz, suggesting that the interfaces ar quite sharp. In the case of rough interfaces the signal has been shown to extend at least down to 120 MHz.[20] Moreover, the NMR intensity between 165 and 210 MHZ (purely interfacial signal) corresponds to almost 1 AL of Co per interface as expected for sharp interfaces. The wide frequency range on which the interfacial signal is spread can be explained by the variety of interfaces which can be encountered in those samples: fcc Co with Cu or Au neighbors, and hcp Co with Cu or Au neighbors also, i.e., four different lines with as many different resonance frequencies. Possible hydrogen release during Co electrodeposition does not seem to play an important role since NMR spectra and therefore the proportion of fcc to hcp structures are not altered for a much lower pH of 1 instead of 4.

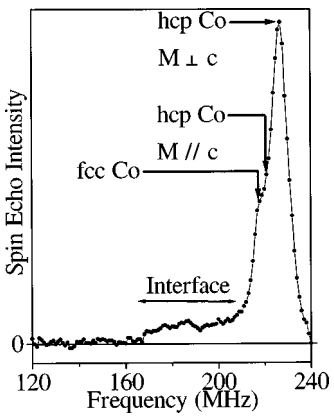

FIG. 2. NMR spectrum of Co in the Cu/Co(11 AL)/Au sandwich deposited at $\eta=0.68$ V. For discussion see text.

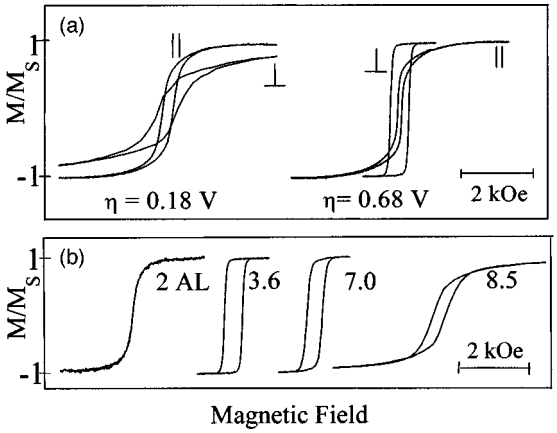

FIG. 3. (a) Hysteresis loops recorded by magneto-optical Kerr effect on a 3.6-Al-thick cobalt film. The magnetic field is applied perpendicular (⊥) and parallel (∥) to the plane. Overpotentials are $\eta=0.18$ and 0.68 V, respectively. (b) Set of polar Kerr hysteresis loops with magnetic field applied perpendicular to the plane for films deposited at $\eta=0.68$ V.

Both magneto-optic Kerr effect measurements and alternating gradient field magnetometry (AGFM) have been used to measure the magnetic hysteresis loops in the configuration with the magnetic field perpendicular and parallel to the film plane. The hysteresis loops of Fig. 3(a) for 3.6-AL-thick Co films obtained at overpotentials of 0.18 and 0.68 V, respectively, reveal two completely different behaviors. At $\eta=0.18$ V the component of the magnetization is strongest along a direction parallel to the film plane. At $\eta=0.68$ V, on the

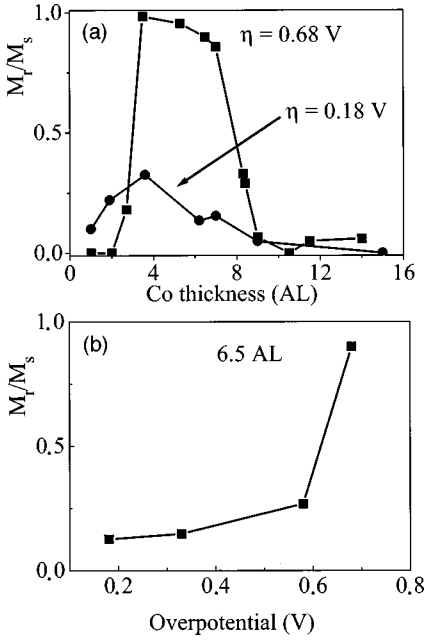

FIG. 4. (a) Ratio of remnant magnetization M_r over saturation magnetization M_s in the perpendicular configuration as a function of film thickness for η=0.18 and 0.68 V. (b) M_r/M_s as a function of η for cobalt films 6.5 AL thick. The continuous increase of M_r/M_s shows the evolution towards fully out-of-plane magnetization at overpotentials $\eta \geqslant 0.68$ V.

other hand, the easy direction of the magnetization is perpendicular to the film plane, as is clear from the rectangular shape of the hysteresis loop. Figure 3(b) shows the evolution of the perpendicular hysteresis loop as a function of film thickness for the films grown η=0.68 V. Quite remarkable is the absence of an open hysteresis loop for $t_{\mathrm{Co}}<2.5$ AL, the sudden opening of the magnetization curve at about 3 AL, and its stretching out above 7 ML. The saturation magnetization $M_s=1375\pm100$ G as measured by AGFM is in good agreement with bulk values.

The ratio of the remnant magnetization $[M_r=M(H=0)]$ in the perpendicular direction over the saturation magnetization M_s, provides a good measure of the tendency of the system to stabilize the out-of-plane configuration. When $M_r/M_s=1$ the magnetization is fully perpendicular. Figure 4(a) shows M_r/M_s as a function of the film thickness t_{Co} for two widely different deposition rates. The ability of high growth rates to stabilize the out-of-plane configuration for 3 AL$<t_{\mathrm{Co}}<$7 AL (M_r/M_s is close to 1) appears clearly while the out-of-plane magnetization is never stable at low deposition rates. The zero value of M_r/M_s for $t_{\mathrm{Co}}<2.5$ AL of films grown at high deposition rates [also reflected in the absence of any hysteresis in the first magnetization curve of Fig. 3(b)] may be due to superparamagnetic islands,[21] with a large size distribution, on the verge of percolation. In contrast, films grown at low deposition rates show ferromagnetic behavior at thicknesses as thin as 1 AL. The drop of M_r/M_s at large t_{Co} is attributed to the fact that shape anisotropy, which tends to align the magnetization in the film plane, overcomes the perpendicular anisotropy. The significant role of overpotential during deposition on the magnetic properties is evidenced by Fig. 4(b) which shows a steep increase of M_r/M_s as a function of overpotential for $\eta>0.6$ V.

Assuming a continuous film with uniaxial anisotropy, the total energy $E=-\mathbf{M}\cdot\mathbf{H}+K_{\mathrm{eff}}\sin^2\vartheta$, where $K_{\mathrm{eff}}$is the effective anisotropy and ϑ is the angle between the magnetization and the normal to the film plane. The anisotropy energy (the second term in the energy) is related to the torque which tends to align the magnetic moments along an easy axis of magnetization. The notion of magnetic anisotropy is fully contained in hysteresis loops like those of Fig. 3 and can be quantified by calculating the area between perpendicular and parallel magnetization curves. The effective anisotropy thus obtained can be viewed as the sum of three terms: $K_{\mathrm{eff}}=K_v+K_s/t_{\mathrm{Co}}-2\pi M_s^2$ (Ref. 9) where K_v is a volume and K_s an interface contribution and $2\pi M_s^2$ is the shape anisotropy. A fitting procedure along the lines described by Beauvillain *et al.*[10] in the regime where the film is continuous provides $K_v=670$ kJ/m^3 and $K_s=0.8$ mJ/m^2. Since in our interpretation we did not consider the second-order term $K_v'\sin^4\vartheta$ to the total energy expression, our K_v value contains both first- and second-order contributions. Our value of K_v, however, is in good agreement with known values obtained by the same analysis for MBE grown films. K_s includes contributions from both the Co/Au and Co/Cu interfaces. The contribution of the Cu coverage to K_s, however, is supposed to be negligible,[10] therefore the value of K_s must be attributed mainly to the Co/Au interface. The negative values obtained for K_{eff} below $t_{\mathrm{Co}}=7$ AL again confirm that the perpendicular orientation of the magnetization is stabilized.

Overpotential controlled nucleation and growth opens up unexpected routes of tailoring the magnetic properties of ultrathin magnetic films. Our results may find applications wherever a control of the magnetic anisotropy needs to be achieved, as in magneto-optic recording media and magnetoresistive sensors. Our main result is that perpendicular magnetization can be induced at high supersaturation (high deposition rates of cobalt) due most probably to a massive formation of small hcp islands for which both crystalline and shape anisotropy contribute to perpendicular magnetization. Anisotropy values calculated by fitting the high supersaturation data are comparable to those obtained for MBE grown films. In future research, the top layer contribution to the interface anisotropy should be investigated in more detail. Certainly more information is needed on the atomic scale growth mechanism of the active layer. In this respect recently developed *in situ* STM on deposition of magnetic films is particularly useful.[18,22]

This work was supported by the Centre National de la Recherche Scientifique (CNRS-ULTIMATECH program).

*Author to whom correspondence should be addressed. Electronic address: bucher@morgane.u-strasbg.fr

[1] See, for example, B. Heinrich and J. A. C. Bland, *Ultrathin Magnetic Structures I and II* (Springer, Berlin, 1994).

[2] J. Switzer *et al.*, Science **264**, 1573 (1994).

[3] M. Alper *et al.*, J. Appl. Phys. **75**, 6543 (1994).

[4] S. K. Lenczowski *et al.*, J. Magn. Magn. Mater. **148**, 455 (1995).

[5] A. Blondel *et al.*, Appl. Phys. Lett. **65**, 3019 (1994).

[6] L. Piraux *et al.*, Appl. Phys. Lett. **65**, 2484 (1994).
[7] W. Schindler and J. Kirschner, Phys. Rev. B **55**, R1989 (1997).
[8] C. Chappert *et al.*, J. Magn. Magn. Mater. **54**, 795 (1986).
[9] C. Chappert and P. Bruno, J. Appl. Phys. **64**, 5736 (1988).
[10] P. Beauvillain *et al.*, J. Magn. Magn. Mater. **121**, 503 (1993).
[11] J. Ferré *et al.*, Appl. Phys. Lett. **56**, 1586 (1990).
[12] R. Allenspach, M. Stampanoni, and A. Bischof, Phys. Rev. Lett. **65**, 3344 (1990).
[13] M. Speckmann, H. P. Oepen, and H. Ibach, Phys. Rev. Lett. **75**, 2035 (1995).
[14] J. P. Bucher, L. Santesson, and K. Kern, Langmuir **10**, 979 (1994).
[15] G. J. Edens, X. Gao, and J. Weaver, J. Electroanal. Chem. **375**, 357 (1994).
[16] The overpotential $\eta=|U-U_{Co/Co^{2+}}|$ measures the departure from the Nerst potential of the Co/Co^{2+}couple. $U_{Co/Co^{2+}}=-1.02$ V/MSE (potential quoted versus the MSE) we found the onset of Co deposition at $\eta=0.13$ V.
[17] M. H. Hölzle, V. Zwing, and D. M. Kolb, Electrochim. Acta **40**, 1237 (1995), and references therein.
[18] F. A. Möller, O. M. Magnussen, and R. J. Behm, Phys. Rev. Lett. **77**, 5249 (1996).
[19] The leading role played by surface defects (steps), has been emphasized mainly on the basis of *in situ* STM measurements on various systems (Refs. 17 and 18).
[20] P. Panissod *et al.*, Hyperfine Interact. **97/98**, 75 (1996).
[21] I. S. Jacobs and C. P. Bean, in *Magnetism*, edited by G. T. Rado and H. Suhl (Academic, New York, 1963), Vol. III, pp. 271–350.
[22] J. L. Bubendorff *et al.*, Surf. Sci. Lett. (to be published).